Nucleon-nucleon scattering observables from solitary boson exchange potential

L. Jäde and H. V. von Geramb
Theoretische Kernphysik, Universität Hamburg, Luruper Chaussee 149, D-22761 Hamburg, Germany
(Received 16 July 1997)

The one solitary boson exchange potential (OSBEP) is used to evaluate observables of *NN* elastic scattering below pion threshold. In this approach, we use a nonlinear model of self-interacting mesons as a substitution for the commonly used phenomenological form factors. *NN* data support an empirical scaling law between the pion and other meson fields, which suggests a link to QCD and significantly reduces the number of parameters in the boson exchange potential. The analysis of *np* and *pp* observables distinguishes the model by its fit and few adjustable parameters. An outlook to apply OSBEP in πN systems is given. [S0556-2813(98)05202-9]

PACS number(s): 13.75.Cs, 11.10.Lm, 13.75.Gx, 21.30.−x

I. INTRODUCTION

The notion of interacting elementary particles for low- and medium-energy nuclear physics is associated with definitions of potential operators which, inserted into a Lippmann-Schwinger equation, yield the scattering phase shifts and observables. In principle, this potential carries the rich QCD substructure consisting of quarks and gluons and thus may be deduced from some microscopic model. There are a number of models which explicitly refer to QCD and have gained remarkable success describing qualitative features of hadronic interactions [1]. Unfortunately, so far none of these models is able to reach the accuracy of phenomenological boson exchange or inversion potentials [2,3]. These models, however, do not contain any explicit reference to QCD and in the case of boson exchange models use effective baryon and meson fields with phenomenological masses, coupling constants and form factors. It remains astonishing that, with these assumptions, they are able to account for a highly quantitative description of *NN* data below pion production threshold and thus have established themselves as the standard models to be used in nuclear physics. Furthermore, inversion and boson exchange models work equally well for meson-nucleon [4,5] and meson-meson [4,6] interactions. This implies that the potentials remain valid at relative distances of ~ 0.3 fm, which is much smaller than the rms radii of mesons and nucleons themselves and smaller than the QCD bag sizes. It is beyond any doubt that nucleons and mesons are genuine QCD objects and we expect their effects to become distinguishable within relative distances of ~ 1.5 fm. In this context, it is common belief that phenomenological form factors effectively describe the actual QCD dynamics at short distances.

To perform a step towards QCD inspired models, we attempt to replace the conventional form factors by a nonlinear meson dynamics using the one solitary boson exchange potential (OSBEP), which was developed recently by the Hamburg group [7]. From the success of the empirical boson exchange potentials, it seems obvious that chiral symmetry is not dominant in *NN* scattering below 300 MeV [8]. Nonetheless, also a phenomenological low-energy model should be inspired by concepts which ensure chiral symmetry conservation. In this sense, we adopt structures from the linear σ model and develop a dynamics of self-interacting mesons. At this stage, we cannot circumvent chiral symmetry breaking by taking the nonlinearities, masses, and coupling constants as free parameters. Most important, the self-interaction is taken into account persistently at all instances. This is achieved by using meson fields which are quasiclassical analytic solutions of nonlinear field equations. Defining free meson operators, the quantization of these fields is done *a posteriori*. Finally, this model is utilized in the framework of a one boson exchange potential (OBEP), which closely follows the Bonn-B potential [9].

The benefit of this approach is the inclusion of nonlinear effects, leading to meson propagators of finite self-energy, which permits us to replace the form factors in conventional boson exchange potentials. Furthermore, an empirical scaling law was discovered which relates the pion mass and its self-interaction coupling constant with the self-interaction parameters of any of the other mesons used. Confirming our conjecture about reminiscent effects of the microscopic substructure subsumed in the empirical form factors, we interpret this as a hint for an underlying symmetry. An obvious benefit of the scaling law is the practical bisection of the number of adjustable parameters. This is a different approach than pursued by the Bonn-CD [10] or Reidlike Nijmegen potentials [11], which achieve perfect fits with an inflating number of parameters.

A description of the theoretical framework, including technical details, can be found in [7]. Therein, we restricted the analysis to fit *np* SM95 phase shifts only. In the present work, we extend the potential to describe *np* as well as *pp* scattering and calculate scattering observables to be compared with the latest database compiled in SAID [12]. Additionally, we show *np* and *pp* phase shift comparisons for Bonn-B [9], Nijm93 [11], Paris [13], OSBEP, and the analysis SM97 of Arndt *et al.* [14].

This paper is organized as follows. In Sec. II, we give the salient features of OSBEP. The fit of the model parameters to phase shifts is discussed in Sec. III and thereafter, an extensive survey of *np* and *pp* scattering observables is given in Sec. IV. An outlook for application of the nonlinear model to πN scattering, together with a summary, is contained in Sec. V.

II. SOLITARY MESONS

It is a common feature of chiral invariant models that spontaneous symmetry breaking leads to nonlinear terms in

TABLE I. OSBEP parameters.

	π	η	ρ	ω	σ_0	σ_1	δ
S^P	0^-	0^-	1^-	1^-	0^+	0^+	0^+
m_β [MeV]	138.03[a]	548.8	769	782.6	720	550	983
$\frac{g_\beta^2}{4\pi}$	13.75	0.702	1.431	21.07	14.64	8.6619[a]	1.259
	$\alpha_\pi = 0.44065$				$f_\rho/g_\rho = 3.829$		

[a]Values for the pp potential are $m_\pi = 134.9764$ MeV and $g^2_{\sigma_1}/4\pi = 8.5531$.

the mesonic part of a Lagrangian which can be interpreted as a self-interaction [15]. Because of this, a meson Lagrangian with the same structure as the linear σ model for all mesons in the OBE potential is assumed. Altogether, we consider the six mesons $\beta = \pi, \eta, \rho, \omega, \sigma, \delta,$ and a Lagrangian

$$\mathcal{L}_\beta = \frac{1}{2}(\partial_\mu \Phi_\beta \partial^\mu \Phi_\beta - m_\beta^2 \Phi_\beta^2) - \frac{\lambda_1^\beta}{2p+2}\Phi_\beta^{2p+2} - \frac{\lambda_2^\beta}{4p+2}\Phi_\beta^{4p+2} + \mathcal{L}_{\rm int}. \tag{2.1}$$

For mesons with nonzero spin the operator Φ_β is a vector in Minkowski space. The parameter p assumes 1/2 or 1 to distinguish odd and even powered nonlinearities and $\mathcal{L}_{\rm int}$ contains desirable couplings to nucleon and other meson fields. In chiral symmetric models, the self-interaction coupling constants λ_1^β and λ_2^β and the various meson masses are related by symmetry relations. This sounds intriguing but is not practical. In view of the ambiguities contained in Eq. (2.1) and, in particular in $\mathcal{L}_{\rm int}$, it appears wise to restrict oneself first to a quantitative model which allows chiral symmetry breaking. In actual calculations, this implies the permission of free parameters in Eq. (2.1) which are the coupling constants, physical masses, and the nonlinearities λ_i^β. After fitting the parameters to observables, we rely on their nature to effectively restore chiral symmetry *a posteriori* [6].

A. Meson propagation

The Lagrangian (2.1) contains self-interacting mesons and possible couplings between themselves and to nucleons. Following the standard one boson exchange models, we neglect meson-meson correlations and treat the interaction between mesons and nucleons perturbatively. The self-interaction of each meson makes the difference to standard models as it is taken into account in a closed analytic form and persistently, leading to analytical solutions of the nonlinear field equations for each Fourier component of the meson fields in Eq. (2.1). For the explicit form and the quantization of these solutions, dubbed as *solitary meson fields*, we refer to our former publication [7].

The probability for the propagation of solitary mesons can now be defined as the amplitude to create an interacting field at some space-time point x which is annihilated into the vacuum at y. The momentum space amplitudes of the solitary meson propagator then reads

$$iP_\beta(k^2, m_\beta) = \sum_{n=0}^{\infty} [C_n^{1/2p}(w_\beta)]^2 \times \frac{[(m_\beta^p \alpha_1^\beta)^2 - m_\beta^{2p}\alpha_2^\beta]^n (2pn+1)^{2pn-2}}{D_{k,n}^{(\beta)2pn+1}(\vec{k}^2 + M_{n,\beta}^2)^{pn}} \times i\Delta_F(k^2, M_{n,\beta}), \tag{2.2}$$

where we introduced the dimensionless coupling constants

$$\alpha_\beta = \frac{1}{(2m_\beta V)^p}\sqrt{\left(\frac{\lambda_1^\beta}{4(p+1)m_\beta^2}\right)^2 - \frac{\lambda_2^\beta}{4(2p+1)m_\beta^2}},$$

$$\alpha_1^\beta = \frac{\lambda_1^\beta}{4(p+1)m_\beta^2(2m_\beta V)^p}, \tag{2.3}$$

$$\alpha_2^\beta = \frac{\lambda_2^\beta}{4(2p+1)m_\beta^2(2m_\beta V)^{2p}},$$

and

$$w_\beta = \frac{\alpha_1^\beta}{\sqrt{\alpha_1^{\beta 2} - \alpha_2^\beta}}. \tag{2.4}$$

The Feynman propagator

$$i\Delta_F(k^2, M_{n,\beta}) = \frac{i}{k^2 - M_{n,\beta}^2}, \tag{2.5}$$

uses the mass spectrum

$$M_{n,\beta} = (2pn+1)m_\beta.$$

For $p = 1/2$ one gets the amplitude for scalar fields and $p = 1$ describes pseudoscalar particles. Vector mesons require $p = 1$ and each term of the sum is multiplied with the Minkowski tensor

$$\left(-g^{\mu\nu} + \frac{k^\mu k^\nu}{M_{n,v}^2}\right).$$

The series (2.2) converges rapidly and in practical calculations it is sufficient to use $n \leqslant 4$.

The Lorentz invariant normalization $D_{k,n}^{(\beta)}$, which occurs in the propagator (2.2), is obtained from the normalization $D_k^{(\beta)}$ of the solitary meson fields by substituting

$$k^\mu \rightarrow \frac{1}{2pn+1}k^\mu.$$

TABLE II. Deuteron properties.

	Bonn-B [9]	OSBEP	Exp.	Ref.
E_B (MeV)	2.2246	2.22459	2.22458900(22)	[31]
μ_d	0.8514[a]	0.8524[a]	0.857406(1)	[32]
Q_d (fm^2)	0.2783[a]	0.2698[a]	0.2859(3)	[33]
A_S (fm$^{-1/2}$)	0.8860	0.8805	0.8802(20)	[33]
D/S	0.0264	0.0258	0.0256(4)	[34]
r_{RMS} (fm)	1.9688	1.957	1.9627(38)	[33]
P_D (%)	4.99	4.80		

[a]Meson exchange current contributions not included.

At this point, we simplify our model. The linear σ model implies that the nonlinear term associated with λ_2^β in Eq. (2.1) is zero for all mesons despite the scalar σ and δ mesons. Since the former is an effective particle to simulate two-pion exchange and the latter contributes little, it is no disadvantage to put $\lambda_2^\beta=0$, implying $\alpha_2^\beta=0$, for all mesons used. This restriction simplifies our expressions and we notice $\alpha_1^\beta=\alpha_\beta$ which allows to drop the subscripts from λ_1^β and α_1^β.

B. Proper normalization

The momentum dependent normalization $D_k^{(\beta)}$ of the solitary mesons plays an important role and requires a detailed discussion. $D_k^{(\beta)}$ can depend on the four-momentum k^μ and the coupling constant α_β. The following conditions [16] are imposed: (i) all amplitudes are to be Lorentz invariant, (ii) $D_k^{(\beta)}$ is dimensionless, (iii) all Feynman diagrams are to be finite, and (iv) the fields are vanishing for $\alpha_\beta\to 0$.

The amplitude (2.2) has to fulfill on-shell conditions known from renormalization theory [15]. At $k^2=m_\beta^2$, the propagator $iP(k^2,m_\beta)$ has to have a pole with residue i. Defining

$$\Gamma_\beta^{(2)}(k^2)=i[P_\beta(k^2,m_\beta)]^{-1}, \tag{2.6}$$

these conditions can be met using

$$\Gamma_\beta^{(2)}(k^2)|_{k^2=m_\beta^2}=0 \tag{2.7}$$

and

$$\frac{d}{dk^2}\Gamma_\beta^{(2)}(k^2)\bigg|_{k^2=m_\beta^2}=1. \tag{2.8}$$

From Eq. (2.2) it is clear, that $iP(k^2,m_\beta)$ readily fulfills Eq. (2.7). The second condition demands that $D_k^{(\beta)}$ equals one for $k^2=m_\beta^2$.

Furthermore, to obtain finite results for all self-energy diagrams involving solitary mesons, it is sufficient to choose

$$D_k^{(\beta)}=\mathcal{O}(k^2),$$

for spinless particles, and

$$D_k^{(\beta)}=\mathcal{O}(k^4),$$

for vector mesons. In summary, all conditions are met with

$$D_k^{(\beta)}=\left\{1+\left(\frac{1}{\alpha_\beta 4(p+1)(2m_\beta)^p}\right)^{2/p}(\sqrt{\vec{k}^2+m_\beta^2}-k_0)^2\right\}^{S+1}, \tag{2.9}$$

where S denotes the particle spin. With this proper normalization, the solitary meson propagator is completely determined and can be applied in a boson exchange potential.

C. The scaling law

In conventional models, meson exchange is described by a product of a Feynman propagator and an empirical form factor

$$\frac{i}{k^2-m_\beta^2}\left(\frac{\Lambda_\beta^2-m_\beta^2}{\Lambda_\beta^2+\vec{k}^2}\right)^{2n_\beta}. \tag{2.10}$$

Using the proper normalization (2.9), the solitary meson propagator was found to resemble very closely the expression (2.10) used in the Bonn-B potential [9]. This essential result permitted us to drop the phenomenological form factors. The astonishing benefit unfolds when we make this comparison for all mesons. Doing so, one sees an empirical scaling relation for the self-interaction coupling constants [7]

$$\alpha_\beta=\alpha_\pi\sqrt{S+1}\left(\frac{m_\pi}{m_\beta}\right)^p. \tag{2.11}$$

α_π is the only remaining parameter to describe the full meson dynamics. This reduces significantly the number of parameters with respect to Bonn-B potential.

III. *NN* PHASE SHIFTS

In the calculation of *NN* phase shifts, we use the meson masses of the Bonn-B potential. There is some evidence that the πNN coupling constant should have a value below the previously used one $g_\pi^2/4\pi=14.4$. The first indication came from a Nijmegen analysis [17] which suggests $f_{\pi NN}^2=0.0745$ (which yields $g_\pi^2/4\pi=13.79$ with our values for the pion and nucleon mass). Additionally, Arndt and coworkers deduced similar value from their analysis of πN scattering [18]. Since we confirmed their result in an independent analysis [19] and intend to apply OSBEP in πN interactions, we fix the πNN coupling constant to the Arndt value

$$\frac{g_\pi^2}{4\pi}=13.75. \tag{3.1}$$

The parameter α_π and the remaining meson-nucleon coupling constants then yield a total number of eight adjustable parameters.

As in the first analysis [7], we started our fitting procedure with *np* phase shifts [14] and deuteron properties, disregarding *pp* data. In this case, we are free of Coulomb effects and there are more partial waves due to the isoscalar and isovector contributions. In this work, the *pp* data were also considered. This required to replace (i) the average nucleon mass 938.926 MeV by the proton mass 938.272 MeV, (ii) the average pion mass 138.03 MeV by the π^0 mass 134.98 MeV. Additionally, the σ_1 coupling constant was reduced by

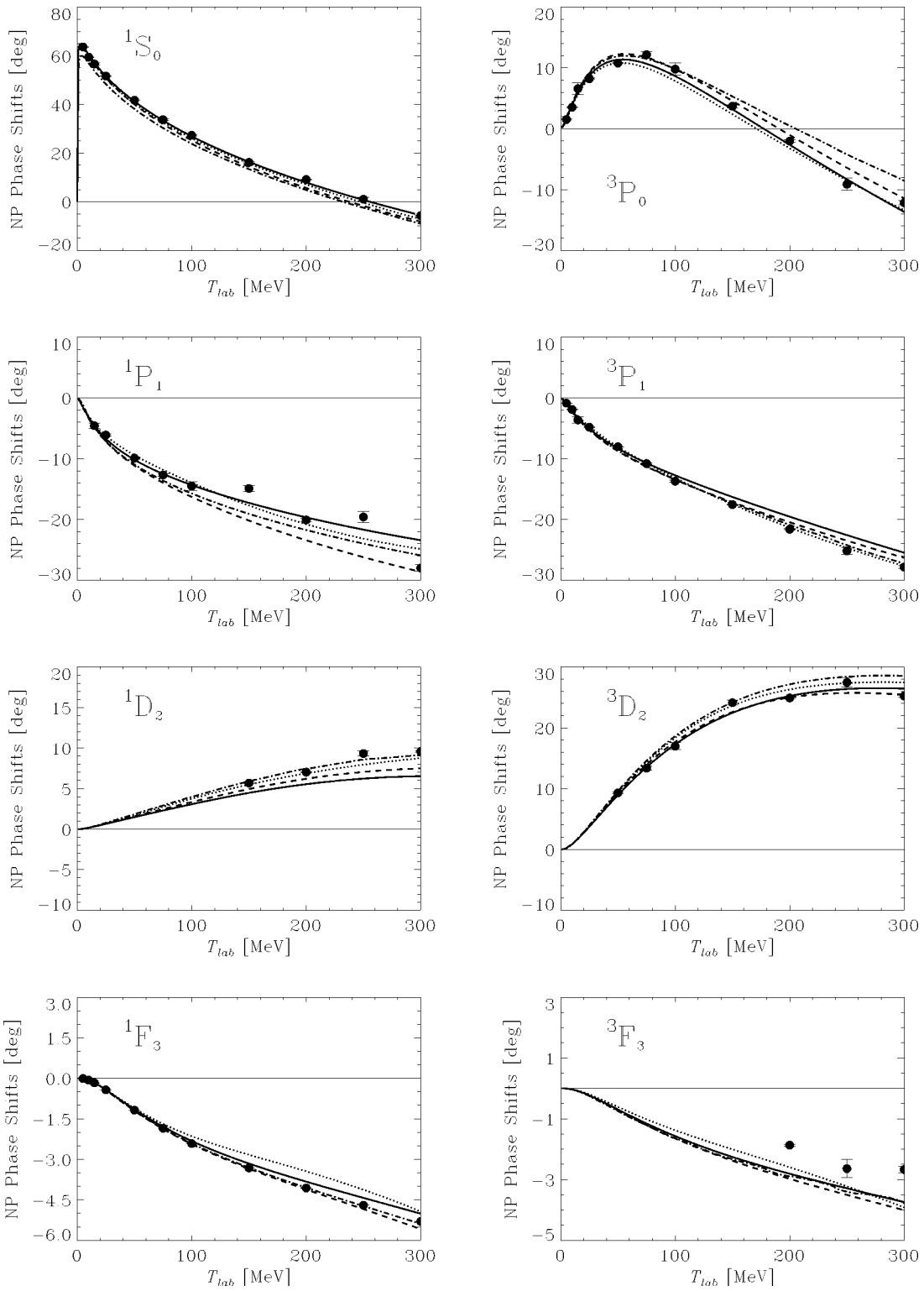

FIG. 1. *np* phase shifts. We show the Arndt SM97 [12] phase shift analysis (circles) compared to the potentials Nijm93 (dotted), Bonn-B (dashed), Paris (dash-dotted), and OSBEP (full).

1.3 % from its *np* value. A static point charge Coulomb potential was included using the Vincent-Phatak method to calculate the Coulomb distorted hadronic phase shifts [20].

The final parameter set is listed in Table I. Deuteron properties are very well reproduced and are given in Table II. *np* phase shifts are shown in Figs. 1 and 2 for single and coupled channels, respectively. *pp* phases are contained in Fig. 3. We plot the results from the Bonn-B, Nijm93, Paris, and OSBEP potential as well as the single energy SM97 analysis. All potentials are in close agreement. Differences, with values of several degrees, do exist for the $^1S_0$ phase shifts of which the Paris potential is the worst. This is true over the whole energy range. Experimentally, the change of sign for *np* lies at $T_{\rm lab}=255.2$ MeV [12]. At 250 MeV, the

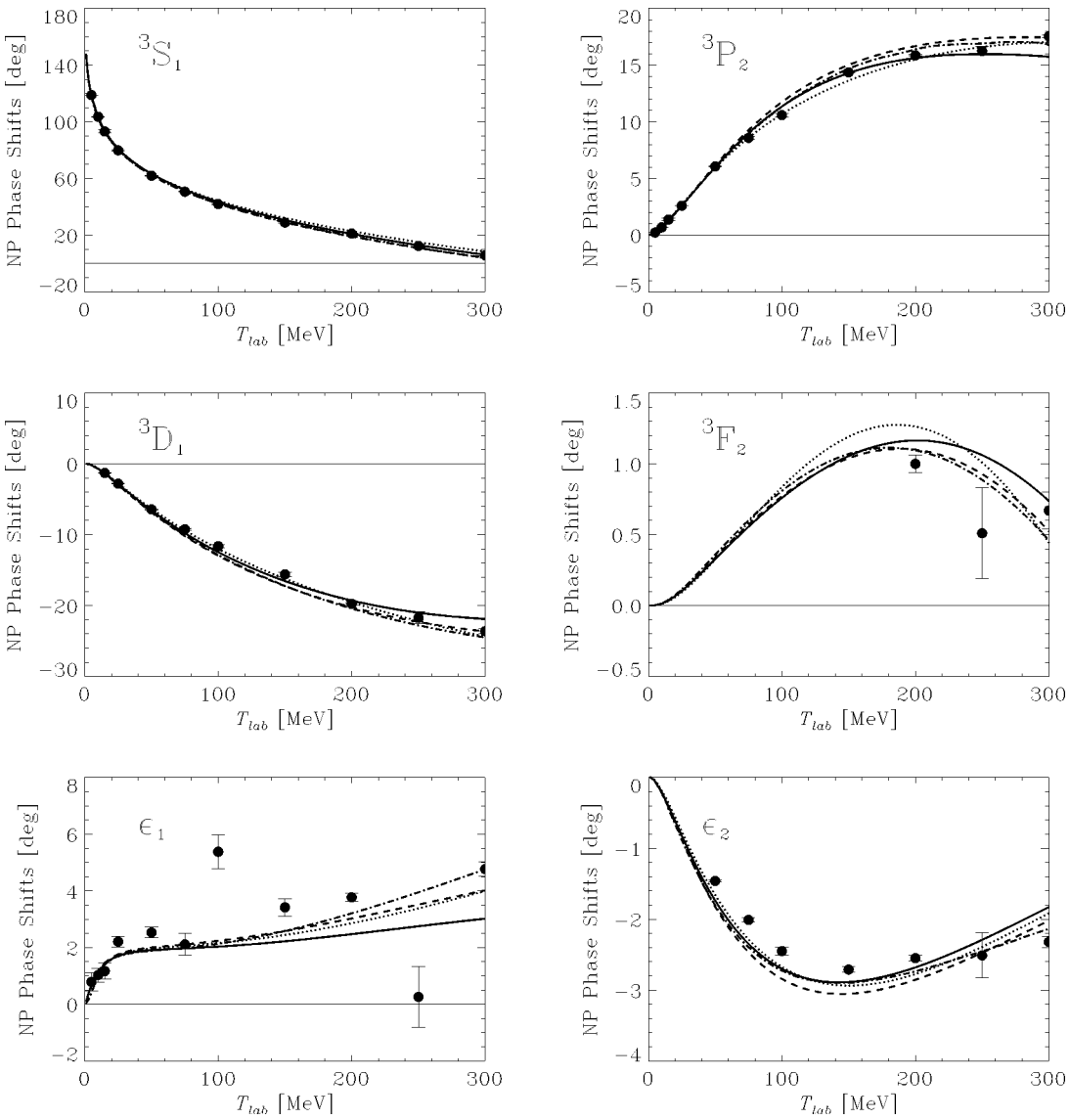

FIG. 2. SYM np phase shifts for the coupled $^3SD_1$ and $^3PF_2$ channels, notations as in Fig. 1.

theoretical values are -2.47 (Paris), -1.72 (Bonn-B), -0.45 (Nijm93), 0.73 (OSBEP), and 1.03 ± 0.84 (SM97). Most striking are the deviations in the P channels. They become crucial at energies above 50 MeV and are visible in the observables. There exist a large amount of literature about these deviations, but a convincing and final solution has not been put forward. In particular, it is known that a potential without $\pi\rho$ correlations leads to an overattraction in the P waves [21]. This can be expected to have a major effect in pp scattering, since isoscalar D waves are absent. It is surprising that, despite the large and consistent database which determines the phase shifts and which is well described by the potential models, there are none the less some strong deviations within the model phase shifts.

Our fitting procedure leaves the coupling constants in qualitative agreement with most Bonn-B values [9]. Differences occur for the πNN and ηNN coupling constants and the tensor to vector ratio κ. We use the experimental value $g_\pi^2/4\pi=13.75$, whereas Bonn-B uses 14.4 which was preferred in the 1980's. Differential cross section data at backward angles support the lower value. SU(3) flavor symmetry relates the πNN and ηNN coupling constants to be

$$\frac{g_\eta^2}{4\pi}=\frac{1}{3}(3-4\alpha_f)^2\,\frac{g_\pi^2}{4\pi}, \tag{3.2}$$

with $\alpha_f\sim0.6-0.65$. This yields $0.7\leqslant g_\eta^2/4\pi\leqslant1.7$, consistent with the value in Table I. More support for the small value can be found in literature [22]. Increasing the ηNN coupling serves to simulate $\pi\rho$ contributions which are generally absent in one boson exchange potentials [21]. In the Bonn-B potential, the value $g_\eta^2/4\pi=3$ is used.

Another feature of our parameter set is the low tensor to vector ratio $\kappa=3.8$ which is in close agreement with the vector-dominance value 3.7, to be compared with $\kappa=6.1$ in Bonn-B. This is reconciled by introducing a direct vector coupling of the photon to the nucleon [21]. We agree with the Nijmegen group that a small πNN coupling constant should be aligned with a value of κ close to the vector dominance value [17].

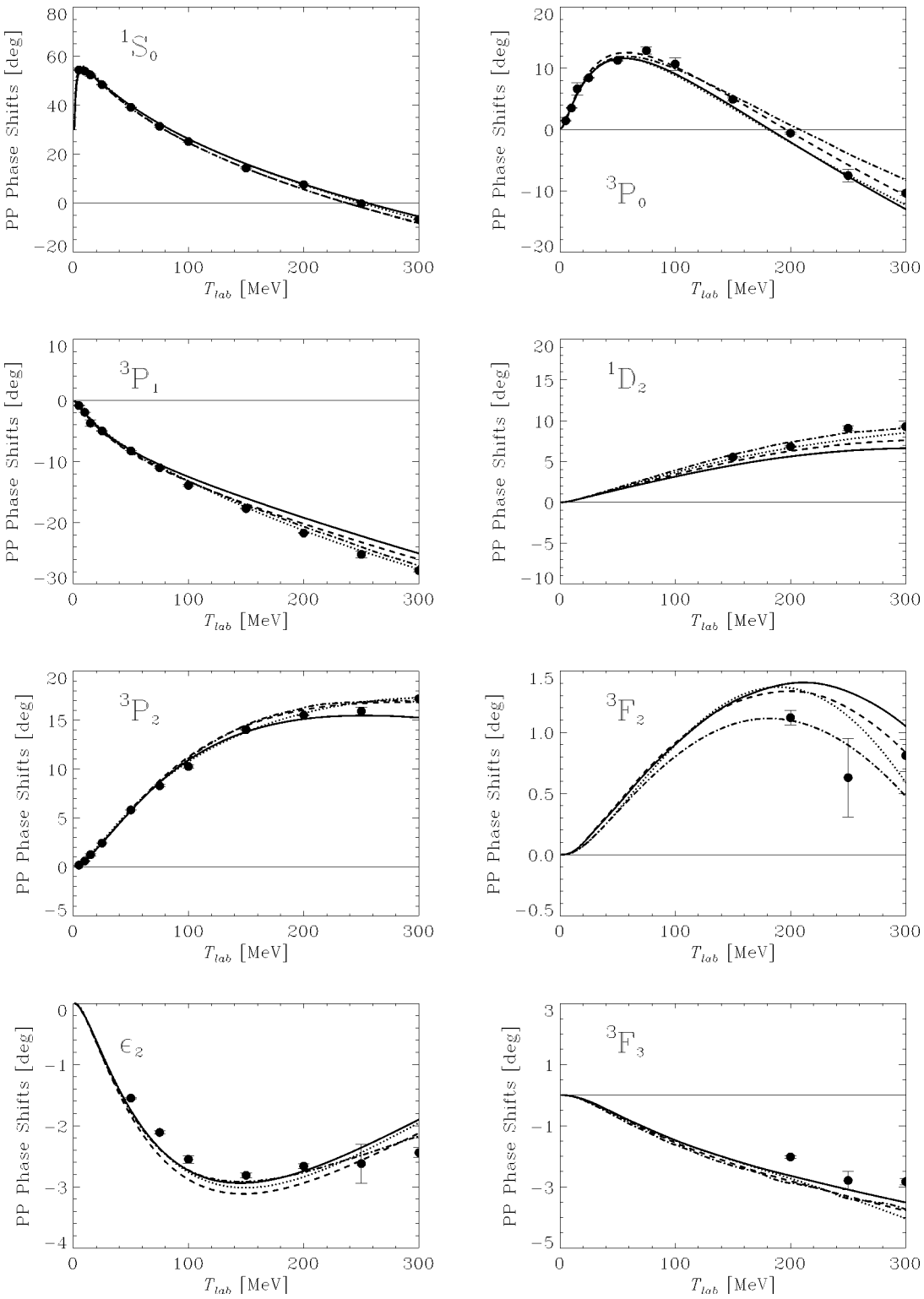

FIG. 3. *pp* phase shifts, notations as in Fig. 1.

IV. OBSERVABLES OF *NN* SCATTERING

To obtain observables from phase shifts we follow the notation of Hoshizaki [23]. The program SAID [12] contains explicitly this option but offers additionally the convention of Bystricky *et al.* [24]. Experimental data with error bars and normalizations together with the theoretical phase shifts for Nijm93 and Paris were taken from SAID. Bonn-B we calculated ourselves and verified its agreement with published values [9].

A. *np* observables

Altogether, there exist 2719 data points for 13 observables between 0 and 300 MeV. Out of 260 possible plots, we selected 19 as representative. They are shown in Figs. 4–7.

TABLE III. χ^2/datum for the OSBEP and several potential models. Data and χ^2 values for the OSBEP, Nijm93, and Paris potential were taken from SAID [12].

Model	No. of param.	np[a]	pp[b]	Total
OSBEP	8	4.1	6.8	5.0
Nijm93	15	5.6	2.2	4.5
Bonn-B	15	12.1	5.8[c]	10.1
Paris	≈60	17.5	2.3	12.6

[a]Energy bin 0–300 MeV (2719 data points).
[b]Energy bin 1–300 MeV (1292 data points).
[c]pp version $g^2_{\sigma_1}/4\pi = 8.8235$, see text.

For each measured observable, we plot the theoretical results of OSBEP (full line), Bonn-B (dashed), Nijm93 (dotted), and Paris (dash-dotted). Visually, the models are hard to distinguish. This is important in view of quite different phase shifts discussed above and significantly different number of adjustable parameters. OSBEP uses about half the parameters of the other models.

However, there are quantitative differences between the models as shown for the χ^2/datum listed in Table III. The table reflects how the database developed during the last years. In the meantime, a number of very precise measurements of differential cross sections and polarization observables became available. In particular, the accurate polarization data at 183 MeV in Fig. 5 from the IUCF group [12] yield large χ^2 contributions for the Nijm93, Paris, and Bonn-B potential whereas the OSBEP agrees very well with these data. Besides that, the differential cross section measurements in Fig. 4, which at large angles are sensitive on the πNN-coupling constant, seem to support the low value of 13.75 used in the OSBEP potential (full line) rather than the older value of 14.4 which is used in the Bonn-B potential (dashed). Therefore, to have a fair comparison, the conventional models should be updated to today's database. As yet, the application in np scattering shows that OSBEP is able to describe the data with comparable accuracy as standard NN potentials using eight parameters only which lends support for the model of solitary mesons and for the scaling law (2.11) in particular.

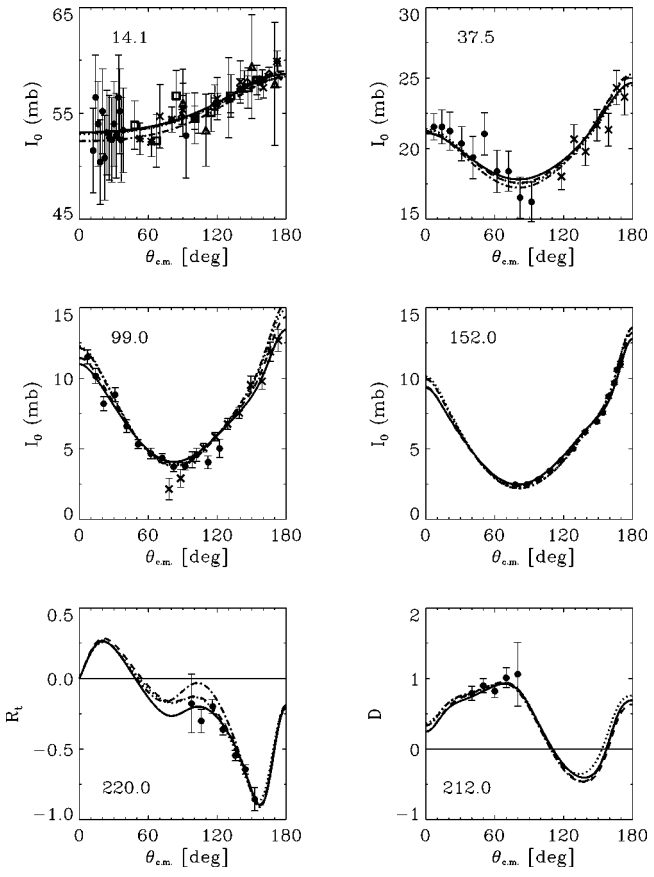

FIG. 4. Observables of np scattering. Kinetic laboratory energy is denoted, experimental data are taken from [12] with notation from [23]. We show theoretical predictions from OSBEP (full) and Bonn-B (dashed), Nijm93 (dotted), and Paris (dashed-dotted).

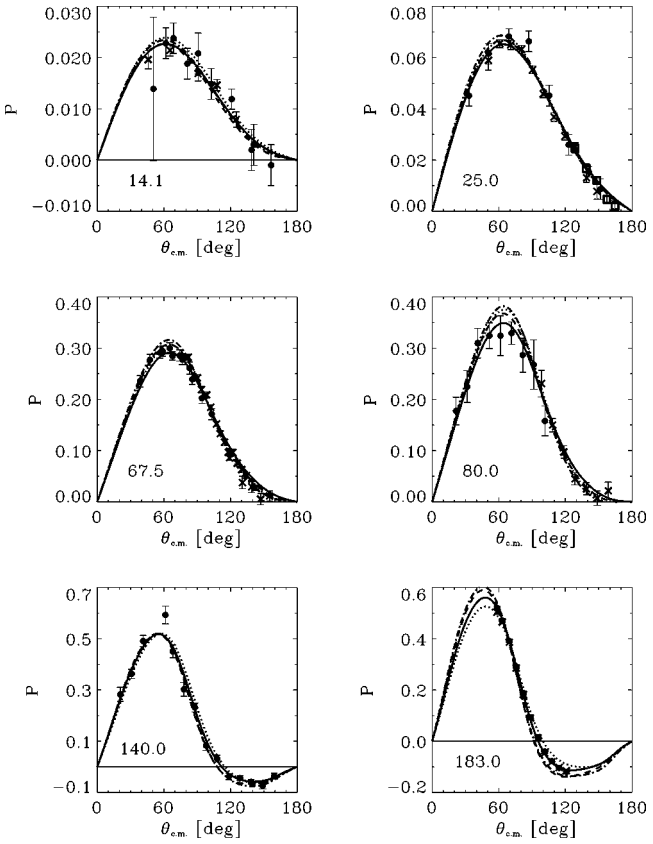

FIG. 5. Observables of np scattering, notations as in Fig. 4.

Besides the general excellent agreement in polarization and spin transfer observables we stress the high accuracy which is obtained in the description of the np spin-correlation parameter A_{zz} at 67.5 MeV, Fig. 6, measured by the Basel group [25]. In this context, Klomp, Stoks, and de Swart [26] argue that a potential which describes A_{zz} at this energy does not allow a high $^3SD_1$ mixing angle ϵ_1 at 50 MeV. Their own PWA, including the Basel data, yields $\epsilon_1 = 2.2° \pm 0.5°$ at this energy. Figure 2 shows that all models considered here predict ϵ_1 slightly below 2°. This must be compared to $\epsilon_1 = 2.9° \pm 0.3°$, a value obtained in a phase shift analysis based on the Basel data [25], and the SM97 value which is $2.53° \pm 0.19°$. We are inclined to follow the arguments of Klomp *et al.* that these values are too large. A similar argument was given by Machleidt and Slaus [27].

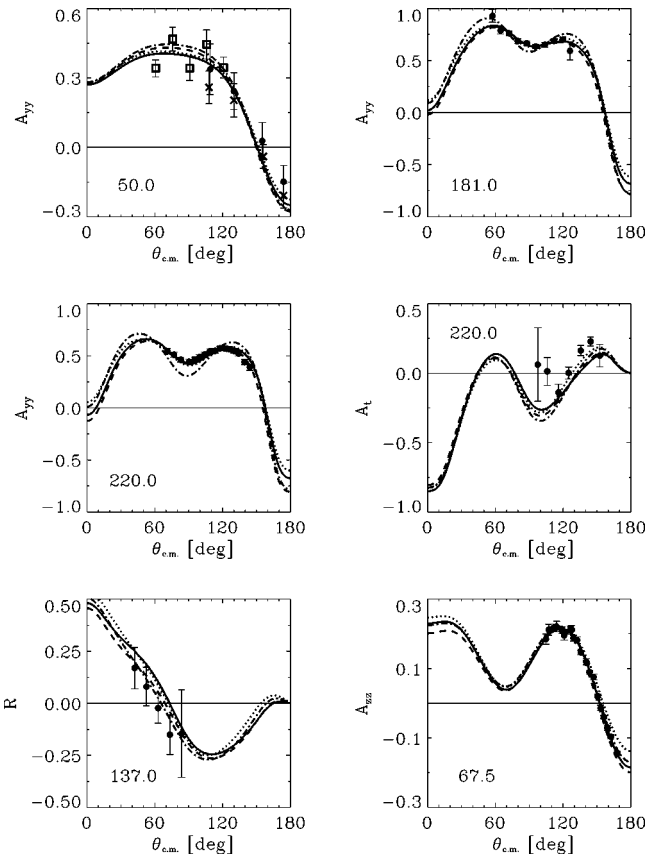

FIG. 6. Observables of np scattering, notations as in Fig. 4.

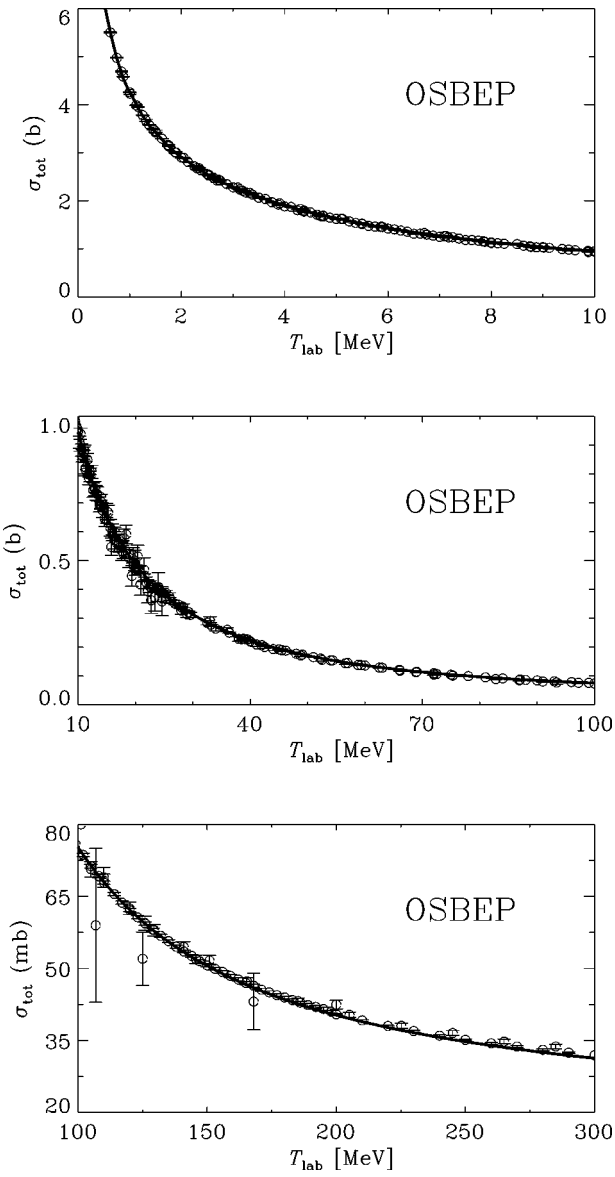

FIG. 7. Total cross section for elastic np scattering.

The total elastic cross section is very well accounted for by OSBEP over the whole energy range, see Fig. 7. The χ^2/datum equals 9.5 for 319 data points below 300 MeV. This value is surprisingly high and not anticipated from Fig. 7. This is mainly due to one dataset only, the experiment of Lisowski *et al.* [28], whose 67 data points are associated with very small error bars, which contributes a χ^2/datum of 39. The remaining 252 $\sigma_{\rm tot}$ measurements are fitted with χ^2/datum of 1.6.

Another quality of fit is obtained by the high-precision NN Bonn-CD [10] and the Reidlike Nijmegen potentials [11]. They sacrifice the simplicity of the original boson exchange potentials and fit each partial wave separately.

B. pp observables

Experimental data cover the interval 1–300 MeV. The data below 1 MeV have been discarded since an assessment of the low-energy data is difficult in the sense that the full electromagnetic interaction has to be taken into account, which is very hard to do in a momentum space calculation. Additionally, these data are associated with very small errors and it is misleading to include them in a χ^2 calculation since they can easily distort the result [29]. After this subtraction, we are left with 1292 data points for 16 observables. In Figs. 8–12, we show 30 plots representative for a total number of 215 possible plots. The Paris potential is still a good fit to the pp data. As the χ^2 in Table III indicates, the quality of OSBEP is not as good as in the case of np scattering. This can be traced to the overattraction of one boson exchange potentials in P channels which signals the lack of $\pi\rho$ correlations in our potential. A more detailed discussion can be found in [21] np data are less seriously affected, since isoscalar contributions partly compensate this shortcoming. We have noticed that a significant improvement is achieved with an artificially large ηNN coupling constant, which contradicts the SU(3) flavor symmetry constraint (3.2). The full Bonn potential includes $\pi\rho$ correlations and neglects η exchange, putting $g_\eta = 0$. The one boson exchange approximation Bonn-B simulates the same contributions by using $/4\pi = 3$. We prefer to use a value $g_\eta^2/4\pi = 0.702$ which agrees with SU(3) symmetry and rely on a more elaborated model, including $\pi\rho$ contributions and Δ isobars, to provide better P-wave phase shifts in a future work.

A pp version of Bonn-B does not exist in literature. We generate a Bonn-B potential suitable for pp analysis by substituting the average nucleon and pion mass of the np version by the proton and π^0 mass, respectively, and including the Coulomb potential into the scattering equation. In addition, we refitted the σ_1 coupling constant to be $g_{\sigma_1}^2/4\pi = 8.8235$. The same prescription was used for OSBEP. Since

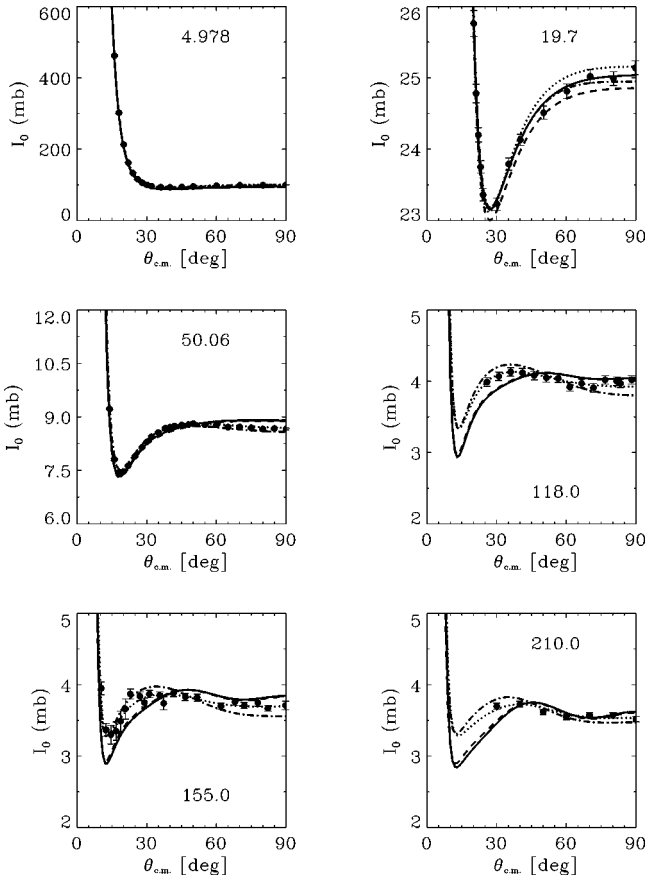

FIG. 8. Observables of pp scattering. Kinetic laboratory energy is denoted, experimental data are taken from [12] with notation from [23]. We show theoretical predictions from OSBEP (full), Bonn-B (dashed, see text), Nijm93 (dotted), and Paris (dashed-dotted).

the main contribution to the large χ^2 comes from the differential cross section in the energy bin 50–150 MeV, we show some of the measured cross sections in Fig. 8. It is obvious, that OSBEP and Bonn-B yield almost the same results, in some of the figures the two curves cannot be distinguished. We obtain a value for the Bonn-B χ^2 which is larger than Nijm93 and Paris but slightly below OSBEP. This is consistent with the enlarged ηNN coupling constant which somewhat compensates the overattraction in the P waves. The remaining harm therefore sticks with the approximations made concerning the meson-meson correlations whereas the model of solitary bosons and the scaling law find the same confirmation as deduced from np.

V. OUTLOOK

With this analysis, we make a comparison of np and pp observables below pion threshold with several potential models. The total χ^2/datum shows the high standard of all models but also some consistent failures. For the one boson exchange potentials, they become obvious for P waves and pp differential cross sections above 80 MeV. This shortcoming is well known from older analyses but is here confirmed and has its cause in the absence of meson-meson correlations. The phenomenological form factors have been consistently replaced by properly normalized solitary meson fields

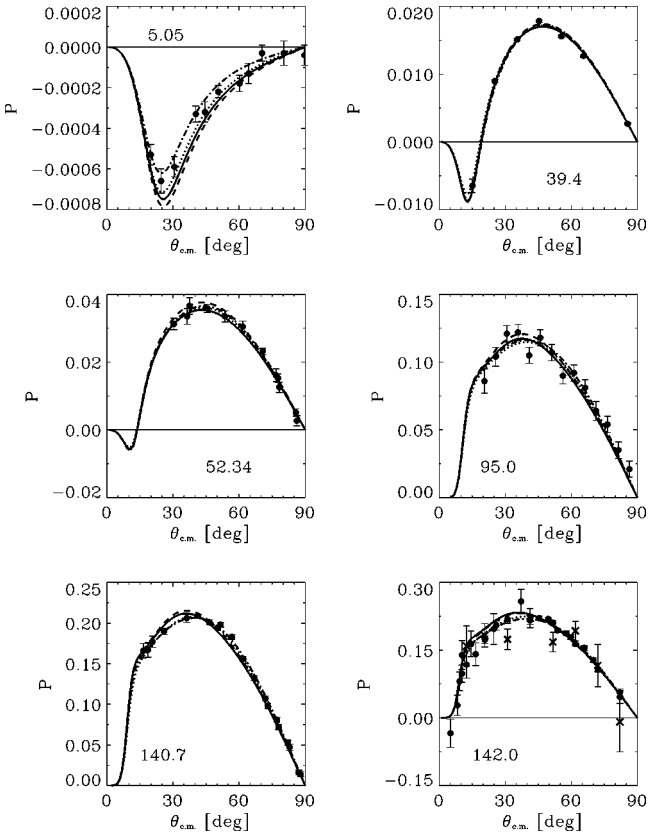

FIG. 9. Observables of pp scattering, notations as in Fig. 8.

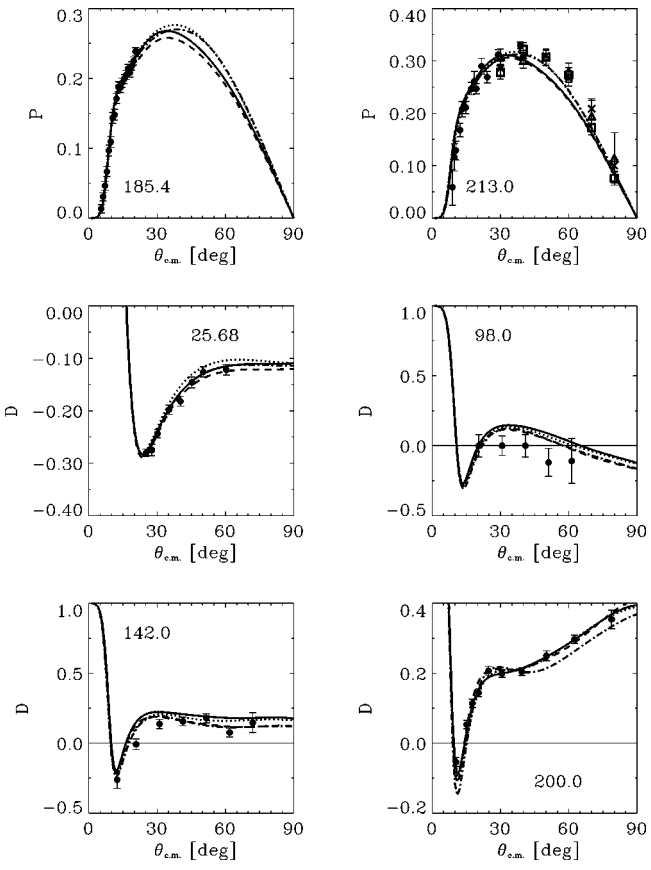

FIG. 10. Observables of pp scattering, notations as in Fig. 8.

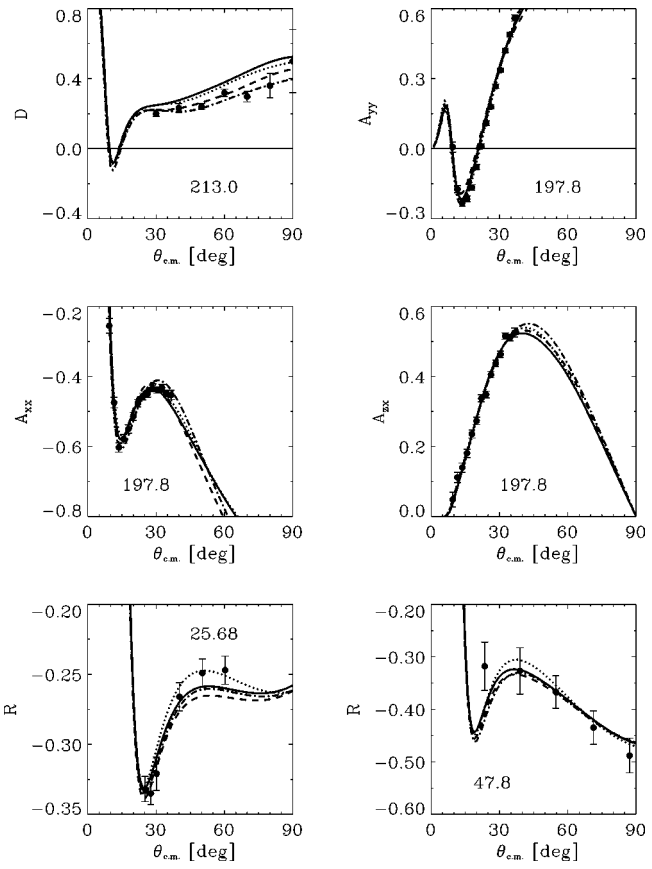

FIG. 11. Observables of pp scattering, notations as in Fig. 8.

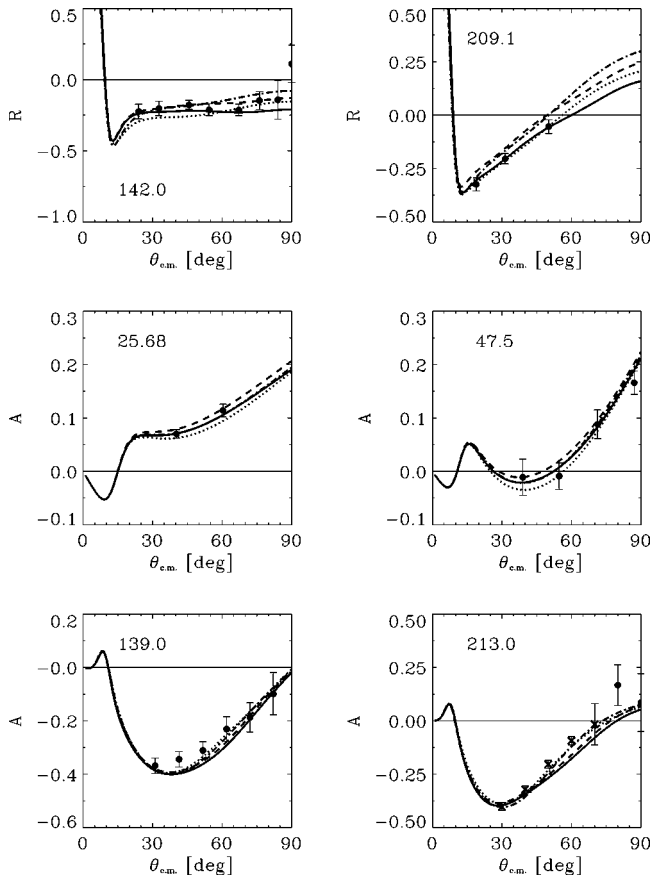

FIG. 12. Observables of pp scattering, notations as in Fig. 8.

which guarantee finite self-energies. An empirical scaling law was deduced from comparison with Bonn-B form factors and this rule was used in case of np and pp data. This issue permitted the reduction of fit parameters to the meson-nucleon coupling constants and one parameter accounting for the meson self-interaction. This study serves the purpose to consistently describe all NN data below pion threshold with the claim to be highly quantitative but with significantly reduced degrees of freedom in the fits. The χ^2/datum results are listed in Table III. The OSBEP result is close to the Nijm93 potential, whereas the Bonn-B and Paris potential yield considerably larger values. However, both models may easily be refitted to improve their χ^2 with respect to the latest database.

As our comparison of several potential models and their predictions for observables of elastic NN scattering shows, there is little room for improvements or to discern model details on-shell. In previous work [30], we made a strong point that $(p,p\gamma)$ bremsstrahlung, triton binding energy, and nucleon-nucleus scattering cannot discern off-shell differences if the on-shell amplitudes are equivalent.

The boson exchange models cannot be extended towards higher energies, the regime of meson production, and hadronic excitations, since this requires a genuine QCD dynamics. New experimental facilities, such as IUCF, CELSIUS, COSY, and TJNAF provide high-quality data and we are seriously considering various potential models suitable for this new domain. Beyond any doubt, this is a subtle problem. Prior to this, it appears interesting to investigate the empirical scaling law in more detail and have a look into the boson exchange model for πN scattering. In this context, it is a common problem that the form factor parametrization of the NN interaction can not be used in the calculation of nucleon pole diagrams [5]. This may be the reason for the failure of the attempts to gain a consistent description of NN, πN, and $\pi\pi$ interactions. To achieve this goal would lend support for the proper normalization of solitary meson fields. The higher order diagrams in the πN scattering equations, which need to be regularized by a form factor, are essentially baryon self-energy and vertex correction amplitudes. Since the proper normalization was designed to yield finite results for these diagrams, it is corollary to work also there.

ACKNOWLEDGMENTS

The authors appreciate discussions with M. Sander and would like to thank R. A. Arndt for providing some FORTRAN routines and encoding OSBEP into SAID. One of us (L. J.) thanks B. Apagyi for his hospitality at the Technical University of Budapest. This work was supported in part by Forschungszentrum Jülich GmbH under Grant No. 41126865.

[1] T. H. R. Skyrme, Nucl. Phys. **31**, 556 (1962); S. Weinberg, Phys. Rev. Lett. **18**, 188 (1967); J. Wambach, in *Quantum Inversion Theory and Applications*, edited by H. V. von Geramb, Lecture Notes in Physics Vol. 427 (Springer, New York, 1994); C. Ordóñez, L. Ray, and U. van Kolck, Phys. Rev. Lett. **72**, 1982 (1994); C. M. Shakin, Wei-Dong Sun, and J. Szweda, Phys. Rev. C **52**, 3353 (1995).

[2] M. M. Nagels, T. A. Rijken, and J. J. de Swart, Phys. Rev. D **17**, 768 (1978); M. Lacombe, B. Loiseau, J. M. Richard, R. Vinh Mau, J. Côté, P. Pirès, and R. de Tourreil, Phys. Rev. C **21**, 861 (1980); R. Machleidt, K. Holinde, and C. Elster, Phys. Rep. **149**, 1 (1987).

[3] H. Kohlhoff and H. V. von Geramb, in *Quantum Inversion Theory and Applications* [1]; M. Sander, *Quanteninversion und Hadron-Hadron Wechselwirkungen* (Shaker-Verlag, Aachen, 1997).

[4] M. Sander and H. V. von Geramb, in *Proceedings of the International Conference on Inverse and Algebraic Quantum Scattering Theory*, Lake Balaton, 1996, edited by B. Apagyi, G. Endredi, and P. Levay, Lecture Notes in Physics Vol. 488 (Springer, New York, 1997); also available as nucl-th/9611001, 1996.

[5] C. Lee, S. N. Yang, and T.-S. H. Lee, J. Phys. G **17**, L131 (1991); B. C. Pearce and B. K. Jennings, Nucl. Phys. **A528**, 655 (1991); F. Gross and Y. Surya, Phys. Rev. C **47**, 703 (1993); C. Schütz, J. W. Durso, K. Holinde, and J. Speth, *ibid.* **49**, 2671 (1994).

[6] D. Lohsc, J. W. Durso, K. Holinde, and J. Speth, Nucl. Phys. **A516**, 513 (1990).

[7] L. Jäde and H. V. von Geramb, Phys. Rev. C **55**, 57 (1997).

[8] K. Holinde, in *Physics with GeV-Particle Beams*, edited by H. Machner and K. Sistemich (World Scientific, Singapore, 1995).

[9] R. Machleidt, Adv. Nucl. Phys. **19**, 189 (1989).

[10] R. Machleidt, F. Sammarruca, and Y. Song, Phys. Rev. C **53**, 1483 (1996).

[11] V. G. J. Stoks, R. A. M. Klomp, C. P. F. Terheggen, and J. J. de Swart, Phys. Rev. C **49**, 2950 (1994).

[12] R. A. Arndt *et al.*, SAID program, access via TELNET under clsaid.phys.vt.edu (login: said); german mirror at said-hh.desy.de (login: physics, password. quantum).

[13] M. Lacombe, B. Loiseau, J. M. Richard, R. Vinh Mau, J. Côté, P. Pirès, and R. de Tourreil, Phys. Rev. C **21**, 861 (1980).

[14] R. A. Arndt, C. H. Oh, I. J. Strakovsky, R. J. Workman, and F. Dohrmann, nucl-th/9706003, 1997.

[15] C. Itzykson and J. B. Zuber, *Quantum Field Theory* (McGraw-Hill, New York 1980).

[16] P. B. Burt, *Quantum Mechanics and Nonlinear Waves* (Harwood Academic, New York, 1981).

[17] V. Stoks, R. Timmermans, and J. J. de Swart, Phys. Rev. C **47**, 512 (1993).

[18] R. A. Arndt, R. L. Workman, and M. M. Pavan, Phys. Rev. C **49**, 2729 (1994).

[19] M. Sander and H. V. von Geramb, Phys. Rev. C **56**, 1218 (1997).

[20] C. M. Vincent and S. C. Phatak, Phys. Rev. C **10**, 391 (1974).

[21] R. Machleidt, K. Holinde, and C. Elster, Phys. Rep. **149**, 1 (1987).

[22] M. Kirchbach and L. Tiator, Nucl. Phys. **A604**, 385 (1996).

[23] N. Hoshizaki, Prog. Theor. Phys. Suppl. **42**, 107 (1968).

[24] J. Bystricky, F. Lehar, and F. Winternitz, J. Phys. (France) **39**, 1 (1978); J. Bystricky, C. Lechanoine-Leluc, and F. Lehar, *ibid.* **48**, 199 (187).

[25] M. Hammans *et al.*, Phys. Rev. Lett. **66**, 2293 (1991).

[26] R. A. M. Klomp, V. G. J. Stoks, and J. J. de Swart, Phys. Rev. C **45**, 2023 (1992).

[27] R. Machleidt and I. Slaus, nucl-th/9303022, 1993.

[28] P. W. Lisowski *et al.*, Phys. Rev. Lett. **49**, 255 (1982).

[29] V. G. J. Stoks and J. J. de Swart, Phys. Rev. C **47**, 761 (1993); **52**, 1698 (1995).

[30] L. Jäde, M. Sander, and H. V. von Geramb, in *Proceedings of the International Conference on Inverse and Algebraic Quantum Scattering Theory*, Lake Balaton, 1996, edited by B. Apagyi, G. Endredi, and P. Levay, Lecture Notes in Physics Vol. 488 (Springer, New York, 1997); also available as nucl-th/9609054, 1996.

[31] G. L. Greene, E. G. Kessler, Jr., R. D Deslattes, and H. Boerner, Phys. Rev. Lett. **56**, 819 (1986).

[32] I. Lindgren, in *Alpha-, Beta-, Gamma-Spectroscopy*, edited by K. Siegbahn (North-Holland, Amsterdam 1965), Vol. II.

[33] T. E. O. Ericson, Nucl. Phys. **A416**, 281 (1984).

[34] N. L. Rodning and L. D. Knutson, Phys. Rev. Lett. **57**, 2248 (1986).